Crystal structure and Hirshfeld surface analysis of 1,6-diamino-2-oxo-4-(thiophen-2-yl)-1,2-dihydro-pyridine-3,5-dicarbonitrile

Farid N. Naghiyev,[a] Victor N. Khrustalev,[b,c] Mehmet Akkurt,[d] Ali N. Khalilov,[e,a] Ajaya Bhattarai,[f]* Fuad Sh. Kerimli[a] and İbrahim G. Mamedov[a]

[a]Department of Chemistry, Baku State University, Z. Khalilov str. 23, Az, 1148 Baku, Azerbaijan, [b]Peoples' Friendship University of Russia (RUDN University), Miklukho-Maklay St. 6, Moscow, 117198, Russian Federation, [c]N. D. Zelinsky Institute of Organic Chemistry RAS, Leninsky Prosp. 47, Moscow, 119991, Russian Federation, [d]Department of Physics, Faculty of Sciences, Erciyes University, 38039 Kayseri, Türkiye, [e]"Composite Materials" Scientific Research Center, Azerbaijan State Economic University (UNEC), H. Aliyev str. 135, Az 1063, Baku, Azerbaijan, and [f]Department of Chemistry, M.M.A.M.C (Tribhuvan University) Biratnagar, Nepal. *Correspondence e-mail: ajaya.bhattarai@mmamc.tu.edu.np

The asymmetric unit of the title compound, $C_{11}H_7N_5OS$, contains two independent molecules (1 and 2). The thiophene ring in molecule 2 is rotationally disordered (flip disorder) by *ca* 180° (around the single C—C bond, to which it is attached) over two sites with the site-occupation factors of 0.9 and 0.1. These two orientations of the thiophene ring in molecule 2 are not equivalent. In the crystal, molecules are linked by intermolecular N—H···O and N—H···N hydrogen bonds into ribbons parallel to (022) along the *a* axis. Within the (022) planes, these ribbons are connected by van der Waals interactions and between the (022) planes by N—H···O hydrogen bonds. In molecule 1, Hirshfeld surface analysis showed that the most important contributions to the crystal packing are from N···H/H···N (27.1%), H···H (17.6%), C···H/H···C (13.6%) and O···H/H···O (9.3%) interactions, while in molecule 2, H···H (25.4%) interactions are the most significant contributors to the crystal packing.

1. Chemical context

The various C—C and C—N bond-formation techniques play key roles in organic synthesis (Celik *et al.*, 2023; Chalkha *et al.*, 2023; Tapera *et al.*, 2022; Lakhrissi *et al.*, 2022). The dihydropyridine moiety, comprising heterocycles, demonstrates a wide spectrum of biological activities, such as antitumor, antitubercular, antimicrobial and anti-diabetic (Mohamed *et al.*, 2013; Soliman *et al.*, 2014). On the other hand, a dihydropyridine scaffold is the active structural unit of a variety of natural products, drugs and functional materials. These compounds have found synthetic applications in the construction of many pharmacologically relevant natural alkaloids, such as the isoquinuclidines, ibogaine, mearsine, dioscorine, caldaphinidine D, catharanthine, vinblastine and vincristine (Sharma & Singh, 2017).
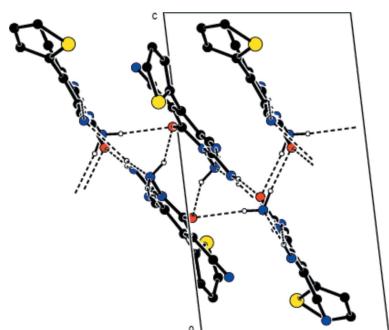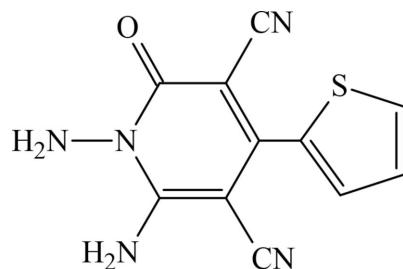
Thus, in the framework of our ongoing structural studies (Maharramov *et al.*, 2021, 2022; Naghiyev *et al.*, 2020, 2021, 2022), we report the crystal structure and Hirshfeld surface analysis of the title compound, 1,6-diamino-2-oxo-4-(thiophen-2-yl)-1,2-dihydropyridine-3,5-dicarbonitrile.

2. Structural commentary

As seen in Fig. 1, the asymmetric unit of the title compound contains two independent molecules (1 and 2). The thiophene ring (S2′/C19/C20′–C22′) in molecule 2 is rotationally disordered (flip disorder) by *ca* 180° (around the single C15—C19 bond to which it is attached) over two sites with the site-occupation factors of 0.9 and 0.1 (fixed after refinement cycles). These two orientations of the thiophene ring in molecule 2 are not equivalent.

In molecule 1, the angle between the thiophene (S1/C8–C11) and pyridine (N1/C2–C6) rings is 50.72 (9)°. In molecule 2, the angle between the two disordered thiophene rings (S2/C19–C22 and S2′/C19/C20′–C22′) is 6.2 (5)°, and they make an angle with the pyridine ring (N6/C13-C17) of 40.3 (1) and 34.8 (5)°, respectively. Molecules 1 and 2 (r.m.s. deviation = 0.126 Å) are almost identical and the geometric parameters are normal and comparable to those of related compounds listed in the *Database survey* section.

Molecules 1 and 2 are stabilized by intramolecular N5—H5*B*···N2 and N10—H10*A*···N7 hydrogen bonds, forming *S*(5) motifs (Table 1; Bernstein *et al.*, 1995).

3. Supramolecular features and Hirshfeld surface analysis

In the crystal, molecules are linked by intermolecular N—H···O and N—H···N hydrogen bonds into ribbons parallel to (022) along the *a*-axis (Table 1, Fig. 2). Within the (022) planes, these ribbons are connected by van der Waals interactions and between the (022) planes by N—H···O intermolecular hydrogen bonds (Table 1, Figs. 3 and 4).
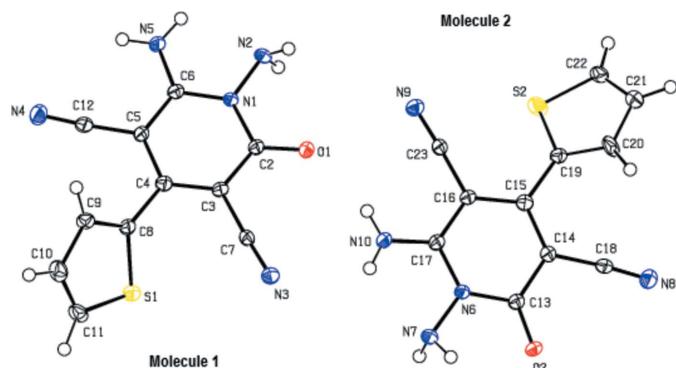
Figure 1
View of the two independent molecules,1 and 2, in the asymmetric unit of the title compound, with displacement ellipsoids for the non-hydrogen atoms drawn at the 30% probability level. For clarity, the minor disordered components in 2 are omitted.
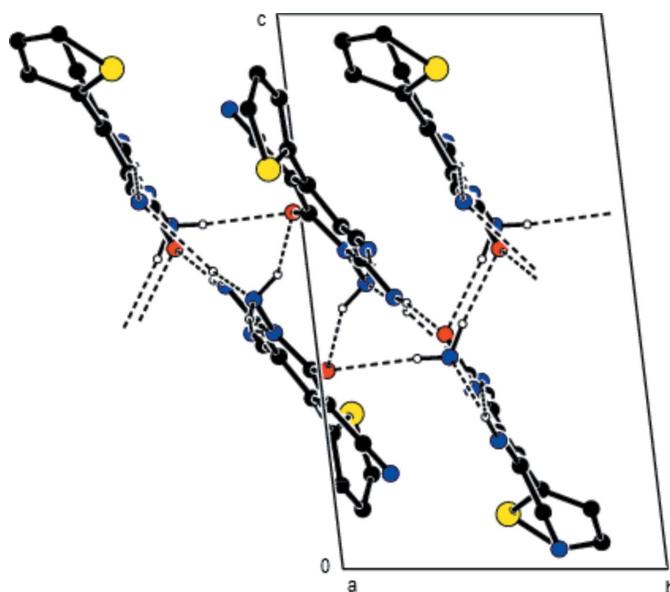
Figure 2
A view of the intermolecular N—H···O and N—H···N interactions along the *a* axis in the crystal structure of the title compound. For clarity, H atoms not involved in hydrogen bonding and disordered components in 2 are omitted.
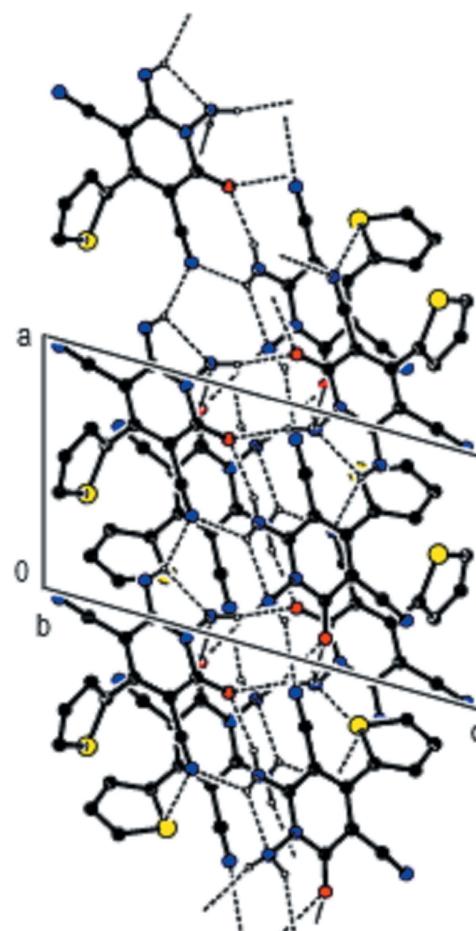
Figure 3
A view of the intermolecular N—H···O and N—H···N interactions along the *b* axis in the crystal structure of the title compound. For clarity, H atoms not involved in hydrogen bonding and disordered components in 2 are omitted.

Table 1
Hydrogen-bond geometry (Å, °).

| D—H···A	D—H	H···A	D···A	D—H···A
N2—H2A···O2^i	0.85 (3)	2.37 (3)	3.212 (2)	174 (2)
N2—H2B···O1^{ii}	0.93 (2)	2.16 (3)	3.086 (2)	169 (2)
N5—H5B···N3^{iii}	0.88 (3)	2.14 (3)	2.944 (2)	151 (2)
N7—H7A···O2^{iv}	0.91 (3)	2.26 (2)	3.010 (2)	139 (2)
N7—H7B···N9^v	0.88 (2)	2.55 (2)	3.348 (2)	152 (2)
N10—H10A···N3	0.85 (2)	2.62 (2)	3.196 (2)	126 (2)
N10—H10B···O1	0.84 (2)	2.11 (3)	2.921 (2)	165 (2)
N5—H5B···N2	0.88 (3)	2.22 (3)	2.606 (2)	106 (2)
N10—H10A···N7	0.85 (3)	2.23 (3)	2.626 (3)	109 (2)

Symmetry codes: (i) $-x + 1, -y, -z + 1$; (ii) $-x + 2, -y + 1, -z + 1$; (iii) $x + 1, y, z$; (iv) $-x, -y, -z + 1$; (v) $x - 1, y, z$.

CrystalExplorer17.5 (Turner *et al.*, 2017) was used to construct Hirshfeld surfaces and generate the related two-dimensional fingerprint plots to illustrate the intermolecular interactions for molecules 1 and 2. The d_{norm} mappings of 1 were conducted in the range -0.5158 to $+1.0500$ a.u. Bright-red circles on the d_{norm} surfaces (Fig. 5a,b) represent N—H···O interaction zones (Table 1). The fingerprint plots of 1 (Fig. 6) show that, while N···H/H···N (27.1%; Fig. 6b) interactions provide the highest contribution (Table 2), as would be expected for a molecule with so many H atoms, H···H (17.6%; Fig. 6c), C···H/H···C (13.6%; Fig. 6d) and O···H/H···O (9.3%; Fig. 6e) contacts are also significant. Table 2 shows the contributions of all contacts. In molecule 2, the d_{norm} mappings were performed in the range -0.5165 to $+1.1535$ a.u. The locations of N—H···O interactions are shown by bright-red circles on the d_{norm} surfaces (Fig. 5c,d), Table 1. Fig. 6 displays the full two-dimensional fingerprint plot and those delineated into the major contacts. H···H interactions (Fig. 6c; 25.4%) are the major factor in the crystal packing with N···H/H···N (Fig. 6b; 24.3%), O···H/H···O (Fig. 6e; 11.7%) and C···H/H···C (Fig. 6d; 11.4%) interactions representing the next highest contributions. The percentage contributions of comparatively weaker interactions in molecules 1 and 2 are given in Table 2. The surroundings of molecules 1 and 2 are quite similar, as seen by the data comparison.

Table 2
Percentage contributions of interatomic contacts to the Hirshfeld surface for the title compound.

Contact	Percentage contribution for molecule 1	Percentage contribution for molecule 2
N···H/H···N	27.1	24.3
H···H	17.6	25.4
C···H/H···C	13.6	11.4
O···H/H···O	9.3	11.7
C···C	7.3	8.5
N···C/C···N	7.0	9.0
S···C/C···S	5.4	1.3
S···H/H···S	5.1	1.8
N···N	2.8	2.7
S···N/N···S	2.2	1.1
O···C/C···O	1.0	1.3
S···S	0.8	0.3
O···N/N···O	0.7	1.2

4. Database survey

A search of the Cambridge Structural Database (CSD, Version 5.42, update of September 2021; Groom *et al.*, 2016) gave thirteen compounds closely related to the title compounds, *viz.* CSD refcodes BEFFOL (**I**; Naghiyev *et al.*, 2022), BEFFUR (**II**; Naghiyev *et al.*, 2022), YAXQAT (**III**; Mamedov *et al.*, 2022), OZAKOS (**IV**; Naghiyev *et al.*, 2021), JEBREQ (**V**; Mohana *et al.*, 2017), JEBRAM (**VI**; Mohana *et al.*, 2017), SETWUK (**VII**; Suresh *et al.*, 2007), SETWOE (**VIII**; Suresh *et al.*, 2007), IQEFOC (**IX**; Naghiyev *et al.*, 2021a), MOKBUL (**X**; Mohamed *et al.*, 2014), PAVQIO (**XI**; Al-Said *et al.*, 2012), YIZGOE01 (**XII**; Jia & Tu, 2008) and YIBZAL (**XIII**; Eyduran *et al.*, 2007).

In the crystal of **I** (monoclinic, $C2/c$), pairs of molecules are linked by pairs of N—H···N hydrogen bonds, forming dimers with an $R_2^2(12)$ ring motif. The dimers are connected by N—H···Br and O—H···O hydrogen bonds, and C—Br···π

Figure 4
A view of the intermolecular N—H···O and N—H···N interactions along the c axis in the crystal structure of the title compound. For clarity, H atoms not involved in hydrogen bonding and the minor disorder components in molecule 2 are omitted.
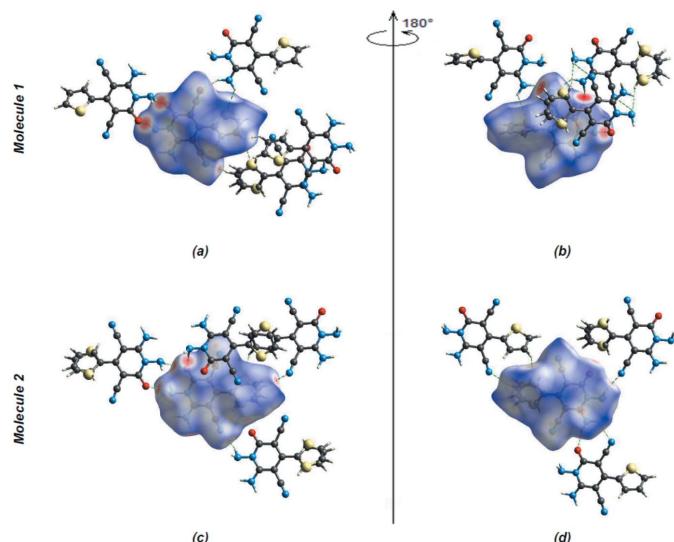

Figure 5
Front (a) and back (b) views of the three-dimensional Hirshfeld surface for molecule 1. Front (c) and back (d) views of the three-dimensional Hirshfeld surface for molecule 2. Some intermolecular N—H···O and N—H···N interactions are shown.
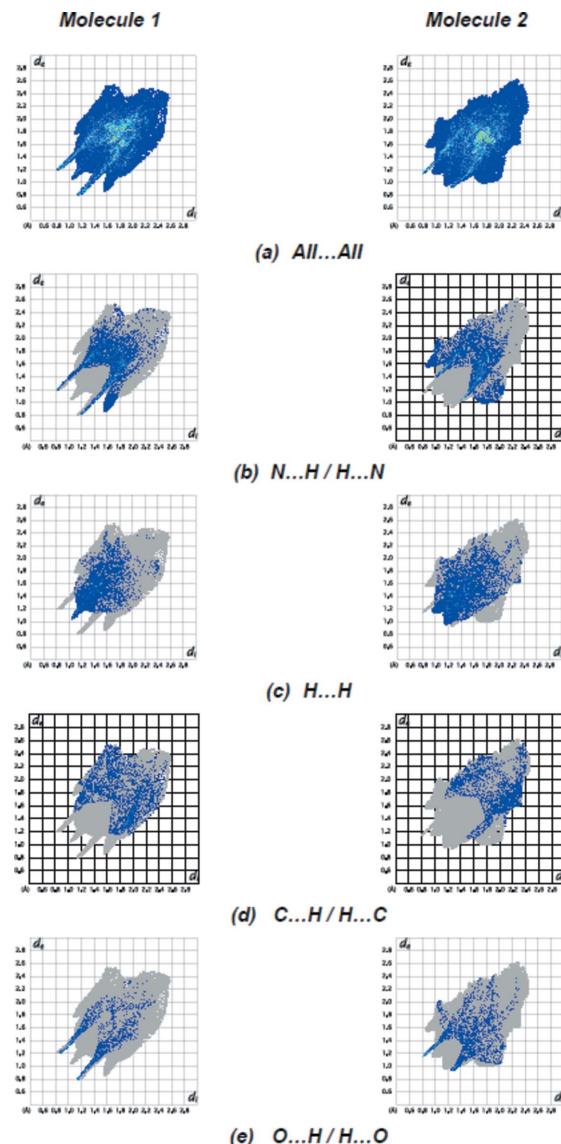
Figure 6
The two-dimensional fingerprint plots for molecules 1 and 2 of the title compound showing (*a*) all interactions, and delineated into (*b*) N···H/H···N, (*c*) H···H, (*d*) C···H/H···C and (*e*) O···H/H···O interactions. The d_i and d_e values are the closest internal and external distances (in Å) from given points on the Hirshfeld surface.

interactions, forming layers parallel to the (010) plane. Compound **II** crystallizes in the triclinic space group $P\bar{1}$ with two independent molecules (**IIA** and **IIB**) in the asymmetric unit. In the crystal of **II**, molecules **IIA** and **IIB** are linked by intermolecular N—H···N and N—H···O hydrogen bonds into layers parallel to (001). These layers are connected along the *c*-axis direction by weak C—H···N contacts. C—H···π and C—N···π interactions connect adjacent molecules, forming chains along the *a*-axis direction. In **III** (space group: *Pc*), the two molecules in the asymmetric unit are joined together by N—H···O hydrogen bonds, forming a dimer with an $R_2^2(16)$ ring motif. N—H···O and N—H···N hydrogen bonds link the dimers, generating chains along the *c*-axis direction, which are connected by C—Br···π interactions. In **IV** (space group: *Pc*), intermolecular N—H···N and C—

H···N hydrogen bonds, as well as N—H···π and C—H···π interactions, connect the molecules in the crystal, generating a 3D network. In both **V** (space group: $P\bar{1}$) and **VI** (space group: $P\bar{1}$), a supramolecular homosynthon [$R_2^2(8)$ ring motif] is formed through N—H···N hydrogen bonds. The molecular structures are further stabilized by π–π stacking, and C—O···π, C—H···O and C—H···Cl interactions. In **VII** (space group: $P2_1/n$), the crystal structure is stabilized by intermolecular C—H···F and C—H···π interactions, and in **VIII** (space group: $P2_1/c$), by intermolecular C—H···O and C—H···π interactions. In **IX** (space group: *Cc*), intermolecular N—H···N and C—H···N hydrogen bonds form molecular sheets parallel to the (110) and (110) planes, crossing each other. Adjacent molecules are further linked by C—H···π interactions, which form zigzag chains propagating parallel to [100]. The compound **X** (space group: $Pca2_1$) crystallizes with two independent molecules in the asymmetric unit. In the crystal, the *A* and *B* molecules are linked by N—H···S, N—H···N and C—H···S hydrogen bonds, forming a three-dimensional network. In **XI** (space group: $P2_1/c$), molecules are linked into a chain along the *b*-axis direction *via* C—H···O interactions. In **XII** (space group: $P\bar{1}$), the crystal packing is consolidated by intermolecular N—H···N, O—H···O and N—H···O hydrogen bonds. In **XIII** (space group: $P2_1/c$), the molecules form centrosymmetric dimers *via* N—H···S hydrogen bonds.

5. Synthesis and crystallization

The title compound was synthesized using a recently reported procedure (Babaee *et al.*, 2020), and colorless crystals were obtained upon recrystallization from an ethanol/water (3:1) solution at room temperature.

6. Refinement

Crystal data, data collection and structure refinement details are summarized in Table 3. The aromatic H atoms were placed at calculated positions (C—H = 0.95 Å) and refined as riding with $U_{iso}(H) = 1.2U_{eq}(C)$. The N-bound H atoms were found in a difference-Fourier map, and refined freely [N2—H2*A* = 0.85 (3), N2—H2*B* = 0.93 (2), N5—H5*A* = 0.87 (3), N5—H5*B* = 0.88 (3), N7—H7*A* = 0.91 (3), N7—H7*B* = 0.88 (2), N10—H10*A* = 0.85 (2) and N10—H10*B* = 0.84 (3) Å], with $U_{iso}(H) = 1.2U_{eq}(N)$. The thiophene ring (S2/C19–C22) in molecule **2** is rotationally disordered (flip disorder) by *ca* 180° (around the single C15—C19 bond, to which it is attached) over two sites with the site-occupation factors of 0.9 and 0.1 (fixed after refinement cycles). A DFIX instruction was applied to constrain the distances in the thiophene rings of disordered molecule **2**. For these rings, FLAT and EADP instructions were also used.

Table 3
Experimental details.

Crystal data	
Chemical formula	$C_{11}H_7N_5OS$
M_r	257.28
Crystal system, space group	Triclinic, $P\bar{1}$
Temperature (K)	100
a, b, c (Å)	8.94782 (10), 9.03908 (9), 14.87299 (18)
α, β, γ (°)	90.9441 (9), 104.1197 (10), 111.7451 (10)
V (Å^3)	1075.92 (2)
Z	4
Radiation type	Cu $K\alpha$
μ (mm^{-1})	2.65
Crystal size (mm)	$0.25 \times 0.20 \times 0.20$
Data collection	
Diffractometer	XtaLAB Synergy, Dualflex, HyPix
Absorption correction	Multi-scan (*CrysAlis PRO*; Rigaku OD, 2021)
T_{min}, T_{max}	0.505, 0.561
No. of measured, independent and observed [$I > 2\sigma(I)$] reflections	32558, 4547, 4467
R_{int}	0.033
$(\sin \theta/\lambda)_{max}$ (Å^{-1})	0.637
Refinement	
$R[F^2 > 2\sigma(F^2)]$, $wR(F^2)$, S	0.040, 0.105, 1.09
No. of reflections	4547
No. of parameters	362
No. of restraints	11
H-atom treatment	H atoms treated by a mixture of independent and constrained refinement
$\Delta\rho_{max}$, $\Delta\rho_{min}$ (e Å^{-3})	0.45, −0.46

Computer programs: *CrysAlis PRO* 1.171.41.117a (Rigaku OD, 2021), *SHELXT* (Sheldrick, 2015a), *SHELXL* (Sheldrick, 2015b), *ORTEP-3 for Windows* (Farrugia, 2012), *PLATON* (Spek, 2020).

ANK, MA and FSK; writing (original draft), MA and ANK; writing (review and editing of the manuscript), MA and ANK; visualization, MA, ANK and IGM; funding acquisition, VNK, AB and ANK; resources, AB, VNK and FSK; supervision, ANK and MA.

References

Al-Said, M. S., Ghorab, M. M., Ghabbour, H. A., Arshad, S. & Fun, H.-K. (2012). *Acta Cryst.* E**68**, o1679.

Babaee, S., Zarei, M., Sepehrmansourie, H., Zolfigol, M. A. & Rostamnia, S. (2020). *ACS Omega*, **5**, 6240–6249.

Bernstein, J., Davis, R. E., Shimoni, L. & Chang, N.-L. (1995). *Angew. Chem. Int. Ed. Engl.* **34**, 1555–1573.

Çelik, M. S., Çetinus, A., Yenidünya, A. F., Çetinkaya, S. & Tüzün, B. (2023). *J. Mol. Struct.* **1272**, 134158.

Chalkha, M., Ameziane el Hassani, A., Nakkabi, A., Tüzün, B., Bakhouch, M., Benjelloun, A. T., Sfaira, M., Saadi, M., Ammari, L. E. & Yazidi, M. E. (2023). *J. Mol. Struct.* **1273**, 134255.

Eyduran, F., Özyürek, C., Dilek, N., Ocak Iskeleli, N. & Şendil, K. (2007). *Acta Cryst.* E**63**, o2415–o2417.

Farrugia, L. J. (2012). *J. Appl. Cryst.* **45**, 849–854.

Groom, C. R., Bruno, I. J., Lightfoot, M. P. & Ward, S. C. (2016). *Acta Cryst.* B**72**, 171–179.

Jia, R. & Tu, S. J. (2008). *Acta Cryst.* E**64**, o1578.

Lakhrissi, Y., Rbaa, M., Tuzun, B., Hichar, A., Anouar, H., Ounine, K., Almalki, F., Hadda, T. B., Zarrouk, A. & Lakhrissi, B. (2022). *J. Mol. Struct.* **1259**, 132683.

Maharramov, A. M., Shikhaliyev, N. G., Zeynalli, N. R., Niyazova, A. A., Garazade, Kh. A. & Shikhaliyeva, I. M. (2021). *UNEC J. Eng. Appl. Sci.* **1**, 5–11.

Maharramov, A. M., Suleymanova, G. T., Qajar, A. M., Niyazova, A. A., Ahmadova, N. E., Shikhaliyeva, I. M., Garazade, Kh. A., Nenajdenko, V. G. & Shikaliyev, N. G. (2022). *UNEC J. Eng. Appl. Sci.* **2**, 64–73.

Mamedov, I. G., Khrustalev, V. N., Akkurt, M., Novikov, A. P., Asgarova, A. R., Aliyeva, K. N. & Akobirshoeva, A. A. (2022). *Acta Cryst.* E**78**, 291–296.

Mohamed, S. K., Akkurt, M., Singh, K., Hussein, B. R. M. & Albayati, M. R. (2014). *Acta Cryst.* E**70**, o993–o994.

Mohamed, S. K., Soliman, A. M., El Remaily, M. A. A. & Abdel-Ghany, H. (2013). *J. Heterocycl. Chem.* **50**, 1425–1430.

Mohana, M., Thomas Muthiah, P. & Butcher, R. J. (2017). *Acta Cryst.* C**73**, 536–540.

Naghiyev, F. N., Akkurt, M., Askerov, R. K., Mamedov, I. G., Rzayev, R. M., Chyrka, T. & Maharramov, A. M. (2020). *Acta Cryst.* E**76**, 720–723.

Naghiyev, F. N., Khrustalev, V. N., Novikov, A. P., Akkurt, M., Rzayev, R. M., Akobirshoeva, A. A. & Mamedov, I. G. (2022). *Acta Cryst.* E**78**, 554–558.

Naghiyev, F. N., Pavlova, A. V., Khrustalev, V. N., Akkurt, M., Khalilov, A. N., Akobirshoeva, A. A. & Mamedov, İ. G. (2021). *Acta Cryst.* E**77**, 930–934.

Rigaku OD (2021). *CrysAlis PRO*. Rigaku Oxford Diffraction, Yarnton, England.

Sharma, V. K. & Singh, S. K. (2017). *RSC Adv.* **7**, 2682–2732.

Sheldrick, G. M. (2015a). *Acta Cryst.* A**71**, 3–8.

Sheldrick, G. M. (2015b). *Acta Cryst.* C**71**, 3–8.

Soliman, A. M., Mohamed, S. K., El-Remaily, M. A. A. & Abdel-Ghany, H. (2014). *J. Heterocycl. Chem.* **51**, 1202–1209.

Spek, A. L. (2020). *Acta Cryst.* E**76**, 1–11.

Suresh, J., Suresh Kumar, R., Perumal, S., Mostad, A. & Natarajan, S. (2007). *Acta Cryst.* C**63**, o141–o144.

Tapera, M., Kekeçmuhammed, H., Tüzün, B., Sarıpınar, E., Koçyiğit, M., Yıldırım, E., Doğan, M. & Zorlu, Y. (2022). *J. Mol. Struct.* **1269**, 133816.

Turner, M. J., McKinnon, J. J., Wolff, S. K., Grimwood, D. J., Spackman, P. R., Jayatilaka, D. & Spackman, M. A. (2017). CrystalExplorer17. The University of Western Australia.

supporting information

Crystal structure and Hirshfeld surface analysis of 1,6-diamino-2-oxo-4-(thiophen-2-yl)-1,2-dihydropyridine-3,5-dicarbonitrile

Farid N. Naghiyev, Victor N. Khrustalev, Mehmet Akkurt, Ali N. Khalilov, Ajaya Bhattarai, Fuad Sh. Kerimli and İbrahim G. Mamedov

Computing details

Data collection: *CrysAlis PRO* 1.171.41.117a (Rigaku OD, 2021); cell refinement: *CrysAlis PRO* 1.171.41.117a (Rigaku OD, 2021); data reduction: *CrysAlis PRO* 1.171.41.117a (Rigaku OD, 2021); program(s) used to solve structure: *SHELXT* (Sheldrick, 2015a); program(s) used to refine structure: *SHELXL* (Sheldrick, 2015b); molecular graphics: *ORTEP-3 for Windows* (Farrugia, 2012); software used to prepare material for publication: *PLATON* (Spek, 2020).

1,6-Diamino-2-oxo-4-(thiophen-2-yl)-1,2-dihydropyridine-3,5-dicarbonitrile

Crystal data

$C_{11}H_7N_5OS$	$Z = 4$
$M_r = 257.28$	$F(000) = 528$
Triclinic, $P\bar{1}$	$D_x = 1.588$ Mg m^{-3}
$a = 8.94782\ (10)$ Å	Cu $K\alpha$ radiation, $\lambda = 1.54184$ Å
$b = 9.03908\ (9)$ Å	Cell parameters from 26181 reflections
$c = 14.87299\ (18)$ Å	$\theta = 3.1$–78.8°
$\alpha = 90.9441\ (9)°$	$\mu = 2.65$ mm^{-1}
$\beta = 104.1197\ (10)°$	$T = 100$ K
$\gamma = 111.7451\ (10)°$	Prism, colourless
$V = 1075.92\ (2)$ Å^3	$0.25 \times 0.20 \times 0.20$ mm

Data collection

XtaLAB Synergy, Dualflex, HyPix diffractometer	4547 independent reflections
Radiation source: micro-focus sealed X-ray tube	4467 reflections with $I > 2\sigma(I)$
φ and ω scans	$R_{int} = 0.033$
Absorption correction: multi-scan (CrysAlisPro; Rigaku OD, 2021)	$\theta_{max} = 79.3°$, $\theta_{min} = 3.1°$
	$h = -11 \rightarrow 11$
	$k = -10 \rightarrow 11$
$T_{min} = 0.505$, $T_{max} = 0.561$	$l = -18 \rightarrow 18$
32558 measured reflections	

Refinement

Refinement on F^2	Primary atom site location: difference Fourier map
Least-squares matrix: full	
$R[F^2 > 2\sigma(F^2)] = 0.040$	Secondary atom site location: difference Fourier map
$wR(F^2) = 0.105$	
$S = 1.09$	Hydrogen site location: mixed
4547 reflections	H atoms treated by a mixture of independent and constrained refinement
362 parameters	
11 restraints	

$w = 1/[\sigma^2(F_o^2) + (0.046P)^2 + 1.11P]$
where $P = (F_o^2 + 2F_c^2)/3$
$(\Delta/\sigma)_{max} = 0.001$
$\Delta\rho_{max} = 0.45$ e Å^{-3}

$\Delta\rho_{min} = -0.46$ e Å^{-3}
Extinction correction: SHELXL,
$Fc^* = kFc[1+0.001\times Fc^2\lambda^3/\sin(2\theta)]^{-1/4}$
Extinction coefficient: 0.0028 (3)

Special details

Geometry. All esds (except the esd in the dihedral angle between two l.s. planes) are estimated using the full covariance matrix. The cell esds are taken into account individually in the estimation of esds in distances, angles and torsion angles; correlations between esds in cell parameters are only used when they are defined by crystal symmetry. An approximate (isotropic) treatment of cell esds is used for estimating esds involving l.s. planes.

Fractional atomic coordinates and isotropic or equivalent isotropic displacement parameters (Å²)

	x	*y*	*z*	U_{iso}*/U_{eq}	Occ. (<1)
S1	0.42276 (5)	0.52922 (6)	0.09865 (3)	0.02122 (13)	
O1	0.79462 (15)	0.40083 (16)	0.42272 (9)	0.0213 (3)	
N1	0.96105 (17)	0.46444 (18)	0.32428 (10)	0.0155 (3)	
N2	1.07380 (19)	0.4068 (2)	0.38163 (11)	0.0204 (3)	
H2A	1.022 (3)	0.306 (3)	0.3791 (16)	0.024*	
H2B	1.100 (3)	0.458 (3)	0.4416 (17)	0.024*	
N3	0.44940 (19)	0.4937 (2)	0.33818 (11)	0.0234 (3)	
N4	0.9777 (2)	0.6738 (2)	0.03594 (12)	0.0287 (4)	
N5	1.14206 (19)	0.5269 (2)	0.23148 (11)	0.0209 (3)	
H5A	1.166 (3)	0.560 (3)	0.1804 (18)	0.025*	
H5B	1.208 (3)	0.495 (3)	0.2738 (17)	0.025*	
C2	0.8182 (2)	0.4562 (2)	0.34957 (12)	0.0167 (3)	
C3	0.7099 (2)	0.5149 (2)	0.28660 (12)	0.0180 (3)	
C4	0.7451 (2)	0.5773 (2)	0.20585 (12)	0.0178 (3)	
C5	0.8932 (2)	0.5840 (2)	0.18606 (12)	0.0170 (3)	
C6	1.0017 (2)	0.5258 (2)	0.24648 (12)	0.0168 (3)	
C7	0.5643 (2)	0.5051 (2)	0.31343 (12)	0.0181 (3)	
C8	0.6340 (2)	0.6391 (2)	0.14265 (12)	0.0175 (3)	
C9	0.6819 (2)	0.7868 (2)	0.10847 (12)	0.0175 (3)	
H9	0.7933	0.8642	0.1235	0.021*	
C10	0.5435 (3)	0.8072 (2)	0.04835 (14)	0.0249 (4)	
H10	0.5523	0.9018	0.0193	0.030*	
C11	0.3974 (2)	0.6796 (2)	0.03603 (13)	0.0239 (4)	
H11	0.2935	0.6741	−0.0026	0.029*	
C12	0.9363 (2)	0.6369 (2)	0.10243 (13)	0.0202 (4)	
S2	0.80863 (7)	−0.08316 (7)	0.72047 (4)	0.02529 (14)	0.9
S2′	0.6895 (15)	−0.0343 (17)	0.8718 (3)	0.0314 (5)	0.1
O2	0.11544 (15)	−0.02340 (16)	0.64254 (9)	0.0214 (3)	
N6	0.31497 (17)	0.12527 (18)	0.57464 (10)	0.0160 (3)	
N7	0.19787 (19)	0.1759 (2)	0.51471 (11)	0.0193 (3)	
H7A	0.129 (3)	0.094 (3)	0.4695 (17)	0.023*	
H7B	0.140 (3)	0.197 (3)	0.5497 (16)	0.023*	
N8	0.2765 (2)	−0.1813 (2)	0.82807 (11)	0.0230 (3)	
N9	0.86800 (19)	0.19394 (19)	0.57542 (11)	0.0213 (3)	
N10	0.4975 (2)	0.25717 (19)	0.48991 (11)	0.0190 (3)	

H10A	0.424 (3)	0.292 (3)	0.4638 (16)	0.023*	
H10B	0.591 (3)	0.293 (3)	0.4796 (16)	0.023*	
C13	0.2627 (2)	0.0251 (2)	0.64097 (12)	0.0174 (3)	
C14	0.3908 (2)	−0.0122 (2)	0.70405 (12)	0.0198 (4)	
C15	0.5502 (2)	0.0312 (2)	0.69219 (12)	0.0194 (4)	
C16	0.5878 (2)	0.1196 (2)	0.61720 (12)	0.0161 (3)	
C17	0.4699 (2)	0.1710 (2)	0.55950 (12)	0.0164 (3)	
C18	0.3323 (2)	−0.1073 (2)	0.77379 (12)	0.0181 (3)	
C19	0.6737 (2)	−0.0168 (2)	0.75586 (11)	0.0189 (3)	
C20	0.6928 (6)	−0.0243 (7)	0.84874 (15)	0.0314 (5)	0.9
H20	0.6287	0.0068	0.8819	0.038*	0.9
C21	0.8164 (3)	−0.0824 (3)	0.89227 (16)	0.0287 (5)	0.9
H21	0.8463	−0.0917	0.9571	0.034*	0.9
C22	0.8866 (3)	−0.1231 (3)	0.82943 (14)	0.0211 (4)	0.9
H22	0.9689	−0.1681	0.8445	0.025*	0.9
C20′	0.7887 (14)	−0.0522 (15)	0.7247 (13)	0.02529 (14)	0.1
H20A	0.7989	−0.0491	0.6626	0.030*	0.1
C21′	0.891 (2)	−0.0945 (14)	0.8000 (13)	0.0211 (4)	0.1
H21A	0.9796	−0.1234	0.7924	0.025*	0.1
C22′	0.8558 (11)	−0.0913 (9)	0.8836 (15)	0.0287 (5)	0.1
H22A	0.9139	−0.1166	0.9398	0.034*	0.1
C23	0.7447 (2)	0.1620 (2)	0.59624 (12)	0.0170 (3)	

Atomic displacement parameters (Å²)

	U^{11}	U^{22}	U^{33}	U^{12}	U^{13}	U^{23}
S1	0.0164 (2)	0.0275 (2)	0.0230 (2)	0.01097 (18)	0.00676 (16)	0.00771 (17)
O1	0.0182 (6)	0.0324 (7)	0.0191 (6)	0.0132 (5)	0.0090 (5)	0.0115 (5)
N1	0.0129 (6)	0.0205 (7)	0.0169 (7)	0.0098 (6)	0.0052 (5)	0.0070 (5)
N2	0.0155 (7)	0.0283 (9)	0.0220 (8)	0.0135 (7)	0.0048 (6)	0.0108 (6)
N3	0.0191 (7)	0.0353 (9)	0.0223 (8)	0.0156 (7)	0.0087 (6)	0.0092 (7)
N4	0.0284 (9)	0.0421 (10)	0.0286 (9)	0.0220 (8)	0.0161 (7)	0.0175 (8)
N5	0.0172 (7)	0.0323 (9)	0.0219 (8)	0.0158 (7)	0.0100 (6)	0.0119 (6)
C2	0.0156 (8)	0.0207 (8)	0.0172 (8)	0.0092 (7)	0.0069 (6)	0.0050 (6)
C3	0.0153 (8)	0.0249 (9)	0.0186 (8)	0.0113 (7)	0.0074 (6)	0.0059 (7)
C4	0.0157 (8)	0.0209 (9)	0.0197 (8)	0.0094 (7)	0.0061 (6)	0.0055 (7)
C5	0.0150 (8)	0.0211 (9)	0.0185 (8)	0.0089 (7)	0.0073 (6)	0.0077 (6)
C6	0.0139 (7)	0.0195 (8)	0.0191 (8)	0.0074 (7)	0.0064 (6)	0.0047 (6)
C7	0.0180 (8)	0.0243 (9)	0.0163 (8)	0.0123 (7)	0.0055 (6)	0.0079 (7)
C8	0.0167 (8)	0.0233 (9)	0.0183 (8)	0.0118 (7)	0.0082 (6)	0.0066 (7)
C9	0.0166 (8)	0.0180 (8)	0.0222 (8)	0.0105 (7)	0.0068 (6)	0.0037 (7)
C10	0.0322 (10)	0.0284 (10)	0.0253 (9)	0.0219 (9)	0.0107 (8)	0.0113 (8)
C11	0.0241 (9)	0.0374 (11)	0.0189 (8)	0.0221 (8)	0.0048 (7)	0.0041 (7)
C12	0.0165 (8)	0.0263 (9)	0.0241 (9)	0.0139 (7)	0.0074 (7)	0.0094 (7)
S2	0.0260 (3)	0.0395 (3)	0.0210 (3)	0.0241 (2)	0.00679 (19)	0.0055 (2)
S2′	0.0332 (9)	0.0657 (15)	0.0095 (13)	0.0340 (10)	0.0073 (14)	0.0067 (17)
O2	0.0136 (6)	0.0303 (7)	0.0236 (6)	0.0096 (5)	0.0086 (5)	0.0107 (5)
N6	0.0131 (6)	0.0201 (7)	0.0182 (7)	0.0090 (6)	0.0058 (5)	0.0076 (6)

N7	0.0159 (7)	0.0262 (8)	0.0209 (7)	0.0128 (6)	0.0058 (6)	0.0092 (6)
N8	0.0224 (8)	0.0257 (8)	0.0236 (8)	0.0100 (7)	0.0097 (6)	0.0084 (6)
N9	0.0179 (7)	0.0260 (8)	0.0243 (8)	0.0111 (6)	0.0087 (6)	0.0080 (6)
N10	0.0156 (7)	0.0251 (8)	0.0207 (7)	0.0102 (6)	0.0088 (6)	0.0101 (6)
C13	0.0157 (8)	0.0205 (9)	0.0186 (8)	0.0085 (7)	0.0066 (6)	0.0052 (6)
C14	0.0170 (8)	0.0258 (9)	0.0197 (8)	0.0104 (7)	0.0067 (7)	0.0095 (7)
C15	0.0175 (8)	0.0246 (9)	0.0196 (8)	0.0110 (7)	0.0064 (7)	0.0063 (7)
C16	0.0134 (8)	0.0194 (8)	0.0174 (8)	0.0073 (6)	0.0059 (6)	0.0040 (6)
C17	0.0159 (8)	0.0190 (8)	0.0164 (8)	0.0079 (7)	0.0064 (6)	0.0032 (6)
C18	0.0137 (7)	0.0218 (9)	0.0201 (8)	0.0087 (7)	0.0038 (6)	0.0050 (7)
C19	0.0148 (8)	0.0232 (9)	0.0220 (8)	0.0096 (7)	0.0071 (6)	0.0081 (7)
C20	0.0332 (9)	0.0657 (15)	0.0095 (13)	0.0340 (10)	0.0073 (14)	0.0067 (17)
C21	0.0218 (11)	0.0467 (13)	0.0228 (10)	0.0176 (10)	0.0075 (9)	0.0136 (9)
C22	0.0179 (9)	0.0206 (10)	0.0274 (12)	0.0108 (8)	0.0045 (9)	0.0116 (8)
C20′	0.0260 (3)	0.0395 (3)	0.0210 (3)	0.0241 (2)	0.00679 (19)	0.0055 (2)
C21′	0.0179 (9)	0.0206 (10)	0.0274 (12)	0.0108 (8)	0.0045 (9)	0.0116 (8)
C22′	0.0218 (11)	0.0467 (13)	0.0228 (10)	0.0176 (10)	0.0075 (9)	0.0136 (9)
C23	0.0171 (8)	0.0193 (8)	0.0171 (8)	0.0091 (7)	0.0055 (6)	0.0065 (6)

Geometric parameters (Å, º)

S1—C11	1.713 (2)	O2—C13	1.232 (2)
S1—C8	1.7239 (18)	N6—C17	1.369 (2)
O1—C2	1.237 (2)	N6—C13	1.397 (2)
N1—C6	1.362 (2)	N6—N7	1.4192 (19)
N1—C2	1.395 (2)	N7—H7A	0.91 (3)
N1—N2	1.4148 (19)	N7—H7B	0.88 (2)
N2—H2A	0.85 (3)	N8—C18	1.147 (2)
N2—H2B	0.93 (2)	N9—C23	1.153 (2)
N3—C7	1.145 (2)	N10—C17	1.322 (2)
N4—C12	1.151 (2)	N10—H10A	0.85 (2)
N5—C6	1.325 (2)	N10—H10B	0.84 (3)
N5—H5A	0.87 (3)	C13—C14	1.442 (2)
N5—H5B	0.88 (3)	C14—C15	1.389 (2)
C2—C3	1.433 (2)	C14—C18	1.432 (2)
C3—C4	1.391 (2)	C15—C16	1.417 (2)
C3—C7	1.426 (2)	C15—C19	1.471 (2)
C4—C5	1.406 (2)	C16—C17	1.414 (2)
C4—C8	1.468 (2)	C16—C23	1.427 (2)
C5—C6	1.412 (2)	C19—C20	1.356 (2)
C5—C12	1.429 (2)	C19—C20′	1.360 (3)
C8—C9	1.388 (3)	C20—C21	1.418 (3)
C9—C10	1.415 (2)	C20—H20	0.9500
C9—H9	0.9500	C21—C22	1.360 (2)
C10—C11	1.353 (3)	C21—H21	0.9500
C10—H10	0.9500	C22—H22	0.9500
C11—H11	0.9500	C20′—C21′	1.420 (3)
S2—C22	1.702 (2)	C20′—H20A	0.9500

S2—C19	1.7120 (17)	C21′—C22′	1.359 (3)
S2′—C19	1.711 (3)	C21′—H21A	0.9500
S2′—C22′	1.719 (3)	C22′—H22A	0.9500
C11—S1—C8	91.74 (9)	H7A—N7—H7B	110 (2)
C6—N1—C2	124.17 (14)	C17—N10—H10A	117.1 (16)
C6—N1—N2	116.35 (13)	C17—N10—H10B	121.3 (16)
C2—N1—N2	119.48 (14)	H10A—N10—H10B	120 (2)
N1—N2—H2A	106.5 (16)	O2—C13—N6	119.40 (15)
N1—N2—H2B	105.8 (14)	O2—C13—C14	124.96 (16)
H2A—N2—H2B	111 (2)	N6—C13—C14	115.63 (15)
C6—N5—H5A	118.2 (16)	C15—C14—C18	124.60 (16)
C6—N5—H5B	119.1 (15)	C15—C14—C13	122.10 (16)
H5A—N5—H5B	123 (2)	C18—C14—C13	113.12 (15)
O1—C2—N1	118.98 (15)	C14—C15—C16	118.19 (15)
O1—C2—C3	125.41 (15)	C14—C15—C19	119.86 (15)
N1—C2—C3	115.61 (14)	C16—C15—C19	121.94 (15)
C4—C3—C7	122.82 (15)	C17—C16—C15	121.00 (15)
C4—C3—C2	122.37 (15)	C17—C16—C23	116.69 (15)
C7—C3—C2	114.82 (15)	C15—C16—C23	122.31 (15)
C3—C4—C5	118.57 (15)	N10—C17—N6	117.38 (15)
C3—C4—C8	121.73 (15)	N10—C17—C16	124.41 (16)
C5—C4—C8	119.68 (15)	N6—C17—C16	118.18 (15)
C4—C5—C6	120.31 (15)	N8—C18—C14	175.66 (18)
C4—C5—C12	123.03 (15)	C20—C19—C15	126.3 (2)
C6—C5—C12	116.49 (15)	C20′—C19—C15	120.7 (8)
N5—C6—N1	117.64 (15)	C20′—C19—S2′	113.7 (9)
N5—C6—C5	123.40 (16)	C15—C19—S2′	125.6 (3)
N1—C6—C5	118.96 (15)	C20—C19—S2	109.75 (18)
N3—C7—C3	176.99 (18)	C15—C19—S2	123.87 (12)
C9—C8—C4	126.08 (16)	C19—C20—C21	114.3 (3)
C9—C8—S1	111.33 (13)	C19—C20—H20	122.8
C4—C8—S1	122.57 (13)	C21—C20—H20	122.8
C8—C9—C10	111.33 (16)	C22—C21—C20	111.4 (2)
C8—C9—H9	124.3	C22—C21—H21	124.3
C10—C9—H9	124.3	C20—C21—H21	124.3
C11—C10—C9	113.81 (17)	C21—C22—S2	111.52 (17)
C11—C10—H10	123.1	C21—C22—H22	124.2
C9—C10—H10	123.1	S2—C22—H22	124.2
C10—C11—S1	111.78 (14)	C19—C20′—C21′	109.0 (15)
C10—C11—H11	124.1	C19—C20′—H20A	125.5
S1—C11—H11	124.1	C21′—C20′—H20A	125.5
N4—C12—C5	175.40 (18)	C22′—C21′—C20′	116 (2)
C22—S2—C19	92.90 (9)	C22′—C21′—H21A	121.9
C19—S2′—C22′	91.8 (9)	C20′—C21′—H21A	121.9
C17—N6—C13	124.25 (14)	C21′—C22′—S2′	109.3 (16)
C17—N6—N7	117.12 (14)	C21′—C22′—H22A	125.3
C13—N6—N7	118.50 (13)	S2′—C22′—H22A	125.3

N6—N7—H7A	108.6 (15)	N9—C23—C16	177.12 (19)
N6—N7—H7B	106.1 (15)		
C6—N1—C2—O1	−178.66 (16)	C18—C14—C15—C19	−2.0 (3)
N2—N1—C2—O1	1.2 (2)	C13—C14—C15—C19	−176.95 (17)
C6—N1—C2—C3	1.1 (3)	C14—C15—C16—C17	3.9 (3)
N2—N1—C2—C3	−179.01 (15)	C19—C15—C16—C17	−177.03 (16)
O1—C2—C3—C4	179.29 (18)	C14—C15—C16—C23	−176.47 (17)
N1—C2—C3—C4	−0.5 (3)	C19—C15—C16—C23	2.6 (3)
O1—C2—C3—C7	−0.4 (3)	C13—N6—C17—N10	175.40 (16)
N1—C2—C3—C7	179.81 (16)	N7—N6—C17—N10	−0.6 (2)
C7—C3—C4—C5	179.12 (17)	C13—N6—C17—C16	−2.9 (3)
C2—C3—C4—C5	−0.6 (3)	N7—N6—C17—C16	−178.87 (15)
C7—C3—C4—C8	0.6 (3)	C15—C16—C17—N10	178.19 (17)
C2—C3—C4—C8	−179.13 (17)	C23—C16—C17—N10	−1.5 (3)
C3—C4—C5—C6	1.1 (3)	C15—C16—C17—N6	−3.6 (3)
C8—C4—C5—C6	179.65 (16)	C23—C16—C17—N6	176.68 (15)
C3—C4—C5—C12	176.19 (17)	C14—C15—C19—C20	−36.9 (4)
C8—C4—C5—C12	−5.2 (3)	C16—C15—C19—C20	144.0 (4)
C2—N1—C6—N5	179.57 (16)	C14—C15—C19—C20′	146.3 (6)
N2—N1—C6—N5	−0.3 (2)	C16—C15—C19—C20′	−32.8 (6)
C2—N1—C6—C5	−0.7 (3)	C14—C15—C19—S2′	−33.7 (6)
N2—N1—C6—C5	179.46 (16)	C16—C15—C19—S2′	147.2 (6)
C4—C5—C6—N5	179.26 (18)	C14—C15—C19—S2	139.30 (16)
C12—C5—C6—N5	3.8 (3)	C16—C15—C19—S2	−39.8 (2)
C4—C5—C6—N1	−0.5 (3)	C22′—S2′—C19—C20	−73 (10)
C12—C5—C6—N1	−175.92 (16)	C22′—S2′—C19—C20′	0.00 (9)
C3—C4—C8—C9	129.8 (2)	C22′—S2′—C19—C15	179.99 (5)
C5—C4—C8—C9	−48.7 (3)	C22′—S2′—C19—S2	6.2 (6)
C3—C4—C8—S1	−52.1 (2)	C22—S2—C19—C20	0.9 (3)
C5—C4—C8—S1	129.31 (16)	C22—S2—C19—C20′	120 (7)
C11—S1—C8—C9	−0.62 (14)	C22—S2—C19—C15	−175.83 (17)
C11—S1—C8—C4	−178.91 (15)	C22—S2—C19—S2′	−1.9 (5)
C4—C8—C9—C10	179.27 (16)	C20′—C19—C20—C21	−6.0 (10)
S1—C8—C9—C10	1.05 (19)	C15—C19—C20—C21	177.0 (2)
C8—C9—C10—C11	−1.1 (2)	S2′—C19—C20—C21	102 (10)
C9—C10—C11—S1	0.6 (2)	S2—C19—C20—C21	0.3 (5)
C8—S1—C11—C10	0.01 (15)	C19—C20—C21—C22	−1.8 (5)
C17—N6—C13—O2	−172.12 (17)	C20—C21—C22—S2	2.4 (3)
N7—N6—C13—O2	3.8 (2)	C19—S2—C22—C21	−1.95 (19)
C17—N6—C13—C14	8.5 (2)	C20—C19—C20′—C21′	2.8 (8)
N7—N6—C13—C14	−175.61 (15)	C15—C19—C20′—C21′	−179.99 (8)
O2—C13—C14—C15	172.61 (18)	S2′—C19—C20′—C21′	0.01 (13)
N6—C13—C14—C15	−8.0 (3)	S2—C19—C20′—C21′	−60 (7)
O2—C13—C14—C18	−2.9 (3)	C19—C20′—C21′—C22′	−0.01 (19)
N6—C13—C14—C18	176.52 (15)	C20′—C21′—C22′—S2′	0.01 (18)
C18—C14—C15—C16	177.10 (17)	C19—S2′—C22′—C21′	−0.01 (11)
C13—C14—C15—C16	2.2 (3)		

Hydrogen-bond geometry (Å, º)

D—H···*A*	*D*—H	H···*A*	*D*···*A*	*D*—H···*A*
N2—H2*A*···O2[i]	0.85 (3)	2.37 (3)	3.212 (2)	174 (2)
N2—H2*B*···O1[ii]	0.93 (2)	2.16 (3)	3.086 (2)	169 (2)
N5—H5*B*···N3[iii]	0.88 (3)	2.14 (3)	2.944 (2)	151 (2)
N7—H7*A*···O2[iv]	0.91 (3)	2.26 (2)	3.010 (2)	139 (2)
N7—H7*B*···N9[v]	0.88 (2)	2.55 (2)	3.348 (2)	152 (2)
N10—H10*A*···N3	0.85 (2)	2.62 (2)	3.196 (2)	126 (2)
N10—H10*B*···O1	0.84 (3)	2.11 (3)	2.921 (2)	165 (2)
N5—H5*B*···N2	0.88 (3)	2.22 (3)	2.606 (2)	106 (2)
N10—H10*A*···N7	0.85 (3)	2.23 (3)	2.626 (3)	109 (2)

Symmetry codes: (i) −*x*+1, −*y*, −*z*+1; (ii) −*x*+2, −*y*+1, −*z*+1; (iii) *x*+1, *y*, *z*; (iv) −*x*, −*y*, −*z*+1; (v) *x*−1, *y*, *z*.